ChemComm

COMMUNICATION

View Article Online
View Journal | View Issue

Cite this: *Chem. Commun.*, 2025, **61**, 15409

Received 25th July 2025,
Accepted 29th August 2025

DOI: 10.1039/d5cc04214c

rsc.li/chemcomm

Harnessing anion-driven interfacial chemistry to suppress water reactivity for stable Zn metal anodes

Yu Meng,†[a] Yibing Yang,†[a] Jiapei Li,†[b] Tian Zhang,[b] Shaozhuan Huang,[a] Yanwu Zhu,*[c] Wenjun Zhang*[b] and Shuilin Wu*[a]

In this study, we unveil a critical function of anions in tailoring the interfacial water coordination environment and electronic structure at the Zn–electrolyte interface. These features thermodynamically hinder water-induced parasitic reactions, enabling highly reversible Zn plating/stripping. And the optimal electrolyte supports high-mass-loading applications in Zn–MnO_2 batteries.

Rechargeable aqueous Zn-ion batteries are considered a promising alternative for large-scale energy storage due to their inherent safety, low cost, and environmental friendliness. The Zn metal anode offers a high theoretical specific capacity (5855 mAh cm^{-3} and 823 mAh g^{-1}) and a low redox potential (−0.76 V *vs.* the standard hydrogen electrode), making it particularly suitable for aqueous battery systems.[1–5] However, the practical application of Zn metal anodes is hindered by parasitic reactions and inhomogeneous Zn deposition.[6] In particular, side reactions such as the hydrogen evolution reaction (HER) and galvanic corrosion of Zn in aqueous electrolytes continuously consume both the electrolyte and active Zn, accelerating the cell failure.[7,8] Furthermore, inhomogeneous Zn plating, including dendrite formation, increases the electrode–electrolyte interfacial area, further facilitating parasitic reactions. These challenges will be intensified at high areal capacities and during extended cycles, posing a significant barrier to achieving a deeply reversible Zn metal anode.[9,10]

These interfacial degradation processes are closely related to the structure and composition of the electrical double layer at the Zn surface, commonly referred to as the Helmholtz layer.[11–14] In conventional mildly acidic electrolytes (*e.g.*, $ZnSO_4$ and $Zn(CF_3SO_3)_2$), water molecules with high polarity preferentially adsorb onto the Zn surface, dominate the Helmholtz plane, and thereby promote hydrogen evolution and Zn corrosion.[16–20] To address this, various electrolyte additives have been employed to tailor the interfacial environment. For instance, molecules with strong Zn affinity, such as sodium 3-mercapto-1-propanesulfonate, pyridine, tetraethyl orthosilicate, and ionic liquids, have been introduced to competitively adsorb on the Zn surface and displace water, forming a water-lean Helmholtz layer.[11,15–22] Similarly, amphiphilic additives have also been employed to create hydrophobic interfacial layers, further inhibiting water access to the Zn surface.[23–25]

Although reducing the water content in the Helmholtz layer can suppress water-induced parasitic reactions, the inherent thermodynamic instability of interfacial water molecules remains a fundamental challenge. This instability arises from the high polarity of water, where strong intramolecular charge separation facilitates electron transfer and accelerates hydrogen evolution.[2,26–28] Notably, the polarity and corresponding electronic structure of interfacial water molecules, which are highly sensitive to the local coordination environment, critically determine the stability of interfacial water molecules.[29] Therefore, understanding these electronic properties and developing new strategies to regulate them is essential for achieving highly reversible Zn metal anodes. While previous studies have established that cations in ionic liquids, such as 1-butyl-3-methylimidazolium ($BMIM^+$), exhibit strong adsorption onto the Zn surface and reconfigure the Helmholtz layer,[11,15,30–34] the role of anions in ionic liquids has been largely overlooked. Actually, the anions are expected to affect the surface chemistry on the Zn surface and also the electrochemical performance of the Zn metal anodes.[35,36] However, the specific contribution of the anionic component has remained largely unexplored. Specifically, their influence on the configurations of ion-water complexation and the electronic structures of interfacial water

[a] *Key Laboratory of Catalysis and Energy Materials Chemistry of Ministry of Education & Hubei Key Laboratory of Catalysis and Materials Science, South-Central Minzu University, Wuhan 430074, China. E-mail: shuilinwu2-c@my.cityu.edu.hk*

[b] *Department of Materials Science and Engineering, and Center of Super-Diamond and Advanced Films, City University of Hong Kong, 83 Tat Chee Avenue, Hong Kong, China. E-mail: apwjzh@cityu.edu.hk*

[c] *A School of Chemistry and Materials Science, University of Science and Technology of China, Hefei, 230026, China. E-mail: zhuyanwu@ustc.edu.cn*

† Yu Meng, Yibing Yang and Jiapei Li contributed equally to this work.

in the Helmholtz layer remain unexplored, representing a significant knowledge gap in interfacial design strategies.

In this study, we elucidate the critical yet overlooked role of anions in $BMIM^+$-based ionic liquid additives for stabilizing interfacial water molecules and the Zn metal anode. Our investigations reveal that these ionic liquids form unique ionic liquid–water complexes that selectively adsorb onto the Zn surface, with the anion dictating two key interfacial properties: local water content and electronic structure of water. Remarkably, BMIM trifluoromethanesulfonate (BMIMOTF) facilitates the formation of a $BMIM(H_2O)_3OTF$ complex with the features of reduced water coordination and an elevated LUMO energy level of water molecules. With the addition of BMIMOTF, the practical Zn–MnO_2 batteries maintain exceptional cycling stability even under high mass loadings (>20 mg cm^{-2}). This work underscores the critical role of electronic characteristics of interfacial water molecules in the Helmholtz layer in governing Zn anode stability and highlights the anion-dependent modulation effect of imidazolium-based ionic liquids as a promising design strategy for high-performance aqueous Zn-ion batteries.

To investigate the impact of anions in imidazole-based ionic liquids on the stability of the Zn metal anode, we first assessed the coulombic efficiency (CE) of Zn-Cu cells using electrolytes containing different anions. As illustrated in Fig. 1a, the addition of BMIMOTF significantly improved the CE, whereas BMIMCl and BMIMTFSI showed negligible enhancements (Fig. 1b and c). We further analyzed the morphology of Zn deposition, and found that, in the 0.5 m $Zn(OTF)_2$ + 0.2 m BMIMOTF electrolyte (Fig. 1d), the plated Zn exhibited a smooth, dense surface, indicating uniform Zn deposition. In contrast, Zn deposited in 0.5 m $ZnCl_2$ + 0.2 m BMIMCl (Fig. 1e) and 1 m $Zn(TFSI)_2$ + 0.2 m BMIMTFSI (Fig. 1f) showed rough, porous morphologies, suggesting that BMIMCl and BMIMTFSI could not effectively regulate the Zn plating behavior. Correspondingly, the Zn foil cycled in the 0.5 m $Zn(OTF)_2$ + 0.2 m BMIMOTF electrolyte showed a smooth and dense surface, while rough, flake-like deposits were observed on Zn foils cycled in 0.5 m $ZnCl_2$ + 0.2 m BMIMCl and 1 m $Zn(TFSI)_2$ + 0.2 m BMIMTFSI electrolytes (Fig. S1, SI). Galvanostatic corrosion tests also demonstrated that BMIMOTF suppressed Zn corrosion much more significantly compared to BMIMCl and BMIMTFSI, as evidenced by the notably reduced corrosion current densities (Fig. 1g and Fig. S2, SI). Moreover, optical microscopy was employed to directly observe hydrogen evolution in the different electrolyte systems (Fig. S3, SI). Pronounced bubble formation was observed in 0.5 m $ZnCl_2$ + 0.2 m BMIMCl and 1 m $Zn(TFSI)_2$ + 0.2 m BMIMTFSI aqueous electrolytes, whereas no visible bubbles were detected in the 0.5 m $Zn(OTF)_2$ + 0.2 m BMIMOTF aqueous electrolyte. Additionally, the electrochemical double-layer capacitance (C') decreased upon the introduction of all ionic liquids (Fig. 1h and Fig. S4, SI), which can be attributed to a reduction in active surface sites due to the characteristic adsorption of ionic liquids on the Zn surface.[14,34,37] This interfacial adsorption also led to a slight increase in charge-transfer resistance in Zn–Zn symmetric cells, as shown by electrochemical impedance spectroscopy (Fig. 1i).[37] The above observations collectively indicate that while all the tested ionic liquids exhibit characteristic adsorption on the Zn surface, their effectiveness in stabilizing the Zn anode varies markedly with the anions in the ionic liquids.

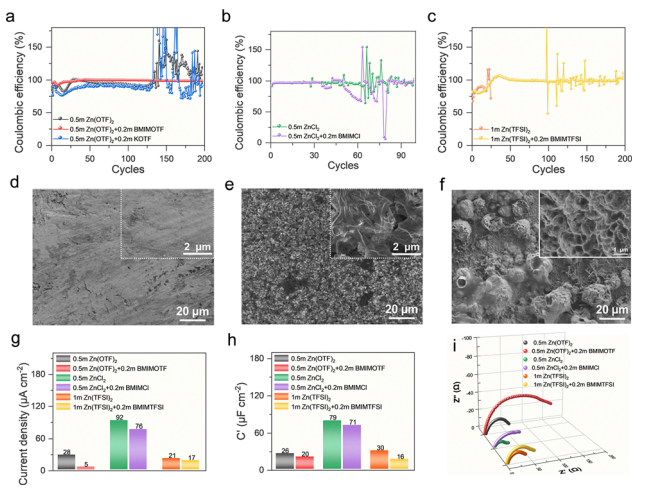

Fig. 1 Electrochemical performance of the Zn metal anode in aqueous electrolytes with different ionic liquids. The coulombic efficiency of repetitive Zn stripping/plating in (a) trifluoromethanesulfonate-based electrolytes, (b) chloride-based electrolytes, and (c) bis(trifluoromethanesulfonyl)imide-based electrolytes. SEM images of plated Zn in (d) 0.5m $Zn(OTF)_2$ + 0.2 m BMIMOTF, (e) 0.5 m $ZnCl_2$ + 0.2 m BMIMCl, and (f) 1 m $Zn(TFSI)_2$ + 0.2 m BMIMTFSI electrolytes. (g) Current densities of galvanic corrosion in different electrolytes. (h) Summary of electrical double-layer capacitance of Zn metal in different electrolytes. (i) Nyquist curves of Zn–Zn cells with different electrolytes.

To understand these variations, we first studied the primary solvation sheath of Zn^{2+} cations in various electrolytes (0.5 m $Zn(OTF)_2$ + 0.2 m BMIMOTF, 0.5 m $Zn(OTF)_2$ + 0.2 m KOTF, 0.5 m $ZnCl_2$ + 0.2 m BMIMCl, and 1 m $Zn(TFSI)_2$ + 0.2 m BMIMTFSI) through Molecular dynamic (MD) simulations. The radial distribution functions (Fig. S5, SI) revealed that changes in electrolyte composition did not affect the primary solvation structures, with six water molecules consistently coordinating around Zn^{2+} cations. This observation was further corroborated by minimal changes in the Fourier transform infrared (FT-IR) spectra (Fig. S6, SI), indicating an intact primary solvation shell around Zn^{2+} cations.[5] These results demonstrate that the incorporation of these ionic liquid additives does not affect the primary solvation environment of Zn^{2+} ions, implying that the observed variations in electrochemical performance are not directly linked to the solvation structure.

We then investigated the evolution of the ionic liquid-induced electrical double-layer on the Zn surface using molecular dynamics (MD) simulations and density functional theory (DFT) calculations. Equilibrium adsorption snapshots from MD simulations for electrolytes containing BMIMOTF, BMIMCl, and BMIMTFSI are shown in Fig. 2a–c. Representative adsorption clusters (*i.e.*, $BMIM^+(H_2O)_3OTF^-$, $BMIM^+(H_2O)_4Cl^-$, and $BMIM^+(H_2O)_4TFSI^-$) are illustrated in Fig. 2d–f with their corresponding electrostatic potential (ESP) maps.[38–40] $BMIM^+(H_2O)_3OTF^-$ exhibited a more dispersive charge distribution, while $BMIM^+(H_2O)_4Cl^-$ and $BMIM^+(H_2O)_4TFSI^-$ displayed more localized charge distributions, consistent with the ESP maps of the pristine ionic liquids (Fig. S7, SI). These

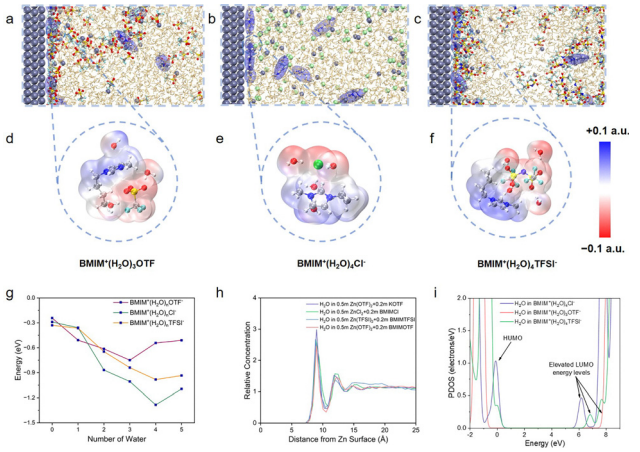

Fig. 2 MD simulation snapshots at the Zn anode interface after 2000 ps for (a) 0.5 m $Zn(OTF)_2$ + 0.2 m BMIMOTF, (b) 0.5 m $ZnCl_2$ + 0.2 m BMIMCl, and (c) 1 m $Zn(TFSI)_2$ + 0.2 m BMIMTFSI electrolytes. (d)–(f) Typical clusters extracted from the MD results, along with their corresponding ESP maps. (g) Formation energies of $BMIM^+(H_2O)_nOTF^-$, $BMIM^+(H_2O)_nCl^-$, and $BMIM^+(H_2O)_nTFSI^-$ clusters with varying water molecules. (h) Distribution statistics of H_2O on the Zn metal anode surface in different electrolytes derived from the MD simulations. (i) PDOS of H_2O in different clusters.

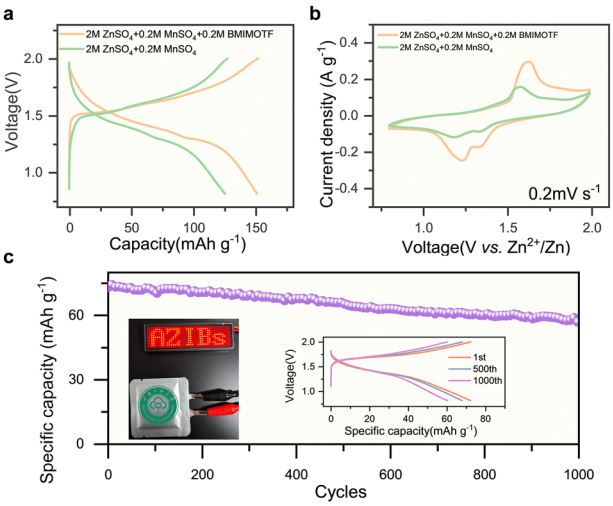

Fig. 3 Electrochemical performance of the Zn-MnO_2 batteries with an areal MnO_2 mass loading of ~20 mg cm^{-2}. (a) Charge–discharge curves of the Zn-MnO_2 cells at 0.1 A g^{-1}, (b) cyclic voltammetry curves at a scan rate of 0.2 mV s^{-1}, and (c) cycling stability of the Zn-MnO_2 cells at 0.8 A g^{-1}, with the inset showing charge–discharge curves for specific cycles.

clusters demonstrated much lower binding energies compared to water molecules on the (002) plane of Zn (Fig. S8, SI), which indicates a stronger adsorption strength of these clusters on the Zn surface. Formation energy analysis (Fig. 2g) revealed that $BMIM^+(H_2O)_3OTF^-$ clusters are thermodynamically more stable than their Cl^- and $TFSI^-$ counterparts, which prefer larger hydration shells (n = 4). This water-lean characteristic of BMIMOTF-based clusters is further supported by the concentration profiles (Fig. 2h), which show reduced water density near the Zn surface. Together, these findings indicate that reducing the water content in the Helmholtz layer can indeed enhance the Zn anode stability, consistent with the superior performance of BMIMOTF. However, despite coordinating with only one additional water molecule, BMIMCl and BMIMTFSI failed to achieve comparable improvements, suggesting that water content alone cannot fully account for the observed differences in electrochemical performance.

To elucidate this discrepancy, we further analyzed the electronic structure of the water molecules within the clusters induced by these ionic liquids, as it fundamentally governs their thermodynamic stability. Projected density of states (PDOS) analysis (Fig. 2i) indicates that $BMIM^+(H_2O)_3OTF^-$ clusters have elevated LUMO energy levels in water molecules, implying reduced electron availability for hydrogen evolution. This LUMO energy elevation can be attributed to the ordered alignment of water molecules induced by the asymmetric yet localized charge distribution of the OTF^- anion. In contrast, both Cl^- (with its high charge density) and $TFSI^-$ (with its symmetric, delocalized charge distribution) tend to induce disordered water orientations, resulting in lower LUMO energy levels and thus greater susceptibility to hydrogen evolution. These insights suggest that BMIMOTF facilitates the formation of a compact, water-deficient Helmholtz layer while simultaneously modulating the electronic structure of interfacial water molecules. These synergistic effects result in effective suppression of parasitic reactions, particularly hydrogen evolution, thereby dramatically enhancing the Zn anode stability. Together, these findings highlight the critical role of the electronic structure of water molecules, along with water content, within the Helmholtz layer in dictating Zn metal anode performance.

To further verify the applicability of the BMIMOTF additive, a Zn–MnO_2 battery was fabricated and evaluated. With BMIMOTF, the cells achieved a higher specific capacity of 150 mAh g^{-1} and an improved discharge plateau compared to cells without the additive, as shown in the galvanostatic charge–discharge curves (Fig. 3a). The CV curves (Fig. 3b) of the Zn-MnO_2 cells with BMIMOTF addition also showed larger areal capacity, indicating that the addition of BMIMOTF enhanced the Zn-ion transfer in the MnO_2 electrode. Additionally, the BMIMOTF-based cell exhibited excellent cycling stability, retaining 80% of its initial capacity after 1000 cycles (Fig. 3c), outperforming BMIMCl-based cells (67% after 300 cycles, Fig. S9, SI). The specific capacity of the cell with BMIMOTF-based electrolyte (76 mAh g^{-1}) is also higher than that of BMIMCl (65 mAh g^{-1}). For BMIMTFSI, poor solubility was observed in the 2 M $ZnSO_4$ aqueous electrolyte. When tested in the 1m $Zn(TFSI)_2$ + 0.2 m BMIMTFSI electrolyte, the Zn–MnO_2 cells showed moderate cycling stability but much lower specific capacity (42 mAh g^{-1}, Fig. S9, SI). EIS measurements (Fig. S10, SI) revealed larger charge-transfer resistances and slower ion diffusion (larger semicircle and lower slope in the low-frequency region) in BMIMCl- and BMIMTFSI-based electrolytes. These results indicate that BMIMCl and BMIMTFSI do not support efficient ion transport under high mass loading, whereas BMIMOTF effectively stabilizes the Zn metal anode and enhances the electrochemical performance of Zn–MnO_2 batteries. Overall, these findings demonstrate the practical applicability of BMIMOTF, especially for cells with high mass loading and areal capacity (Table S1, SI).

This study demonstrates that anion chemistry in $BMIM^+$-based ionic liquids plays a pivotal role in stabilizing interfacial

water within the Helmholtz layer and thereby enabling a highly reversible Zn metal anode. By forming an ion–water complex that modulates the water content and electronic structure, anions critically influence the interfacial stability. Among the systems studied, BMIMOTF promotes the formation of a compact $BMIM(H_2O)_3OTF$ cluster characterized by low water content and an elevated LUMO energy level. These properties promote the stability of interfacial water and contribute to exceptional electrochemical performance: Zn–Cu cells with the 1 m $Zn(OTF)_2$ + 0.2m BMIMOTF electrolyte achieve a high average coulombic efficiency of 99.6% over 400 cycles at 10 mA cm^{-2} with 10 mAh cm^{-2} Zn per cycle. Furthermore, Zn–MnO_2 batteries with the addition of BMIMOTF demonstrate exceptional durability even under high cathode loadings (>20 mg cm^{-2}). These findings highlight the decisive role of interfacial water's electronic structure in dictating Zn anode stability and establishing anion-mediated modulation of water's electronic characteristics as an effective strategy for achieving a deeply reversible Zn metal anode.

This work was supported by the National Natural Science Foundation of China (22209211, 52172241, 52325202, and 52372229), Hong Kong Research Grants Council (CityU 11310123 and CityU 11315622), and the research funds from South-Central Minzu University (YZZ22001).

Conflicts of interest

There are no conflicts to declare.

Data availability

The data supporting this article have been included as part of the SI. See DOI: **https://doi.org/10.1039/d5cc04214c**

Notes and references

1 H. R. Du, Y. H. Dong, Q. J. Li, R. R. Zhao, X. Q. Qi, W. H. Kan, L. M. Suo, L. Qie, J. Li and Y. H. Huang, *Adv. Mater.*, 2023, **35**(25), 2210055.
2 F. Wang, O. Borodin, T. Gao, X. L. Fan, W. Sun, F. D. Han, A. Faraone, J. A. Dura, K. Xu and C. S. Wang, *Nat. Mater.*, 2018, **17**(6), 543.
3 S. L. Wu, Y. T. Chen, T. P. Jiao, J. Zhou, J. Y. Cheng, B. Liu, S. R. Yang, K. L. Zhang and W. J. Zhang, *Adv. Energy Mater.*, 2019, **9**(47), 1902915.
4 J. P. Xie, D. W. Lin, H. Lei, S. L. Wu, J. L. Li, W. J. Mai, P. F. Wang, G. Hong and W. J. Zhang, *Adv. Mater.*, 2024, **36**(17), 2306508.
5 S. L. Wu, Y. B. Yang, M. Z. Sun, T. Zhang, S. Z. Huang, D. H. Zhang, B. L. Huang, P. F. Wang and W. J. Zhang, *Nano-Micro Lett.*, 2024, **16**(1), 161.
6 L. Ma, M. A. Schroeder, O. Borodin, T. P. Pollard, M. S. Ding, C. S. Wang and K. Xu, *Nat. Energy*, 2020, **5**(10), 743–749.
7 J. Zhang, Y. J. Wang, Z. W. Zhao, P. F. Li, G. C. Tang, W. H. Chen and Z. Q. Peng, *Adv. Energy Mater.*, 2024, **14**(34), 2401560.
8 Y. C. Hu, Z. W. Min, G. Y. Zhu, Y. W. Zhang, Y. X. Pei, C. Chen, Y. M. Sun, G. J. Liang and H. M. Cheng, *Nat. Commun.*, 2025, **16**(1), 3255.
9 Y. N. Chen, S. Zhou, J. W. Li, X. Zhang, C. C. Zhou, X. D. Shi, C. X. Zhang, G. Z. Fang, S. Q. Liang and Z. Su, *et al.*, *Angew. Chem., Int. Ed.*, 2025, **64**(18), e202423252.
10 Z. Xu, J. Li, Y. Fu, J. Ba, F. Duan, Y. Wei, C. Wang, K. Zhao and Y. Wang, *Energy Environ. Sci.*, 2025, **18**(9), 4251–4261.
11 G. W. Gao, X. M. Huo, B. X. Li, J. X. Bi, Z. K. Zhou, Z. Z. Du, W. Ai and W. Huang, *Energy Environ. Sci.*, 2024, **17**(20), 7850–7859.
12 N. Hu, W. S. Lv, W. J. Chen, H. Tang, X. Y. Zhang, H. Y. Qin, D. Huang, J. L. Zhu, Z. J. Chen and J. Xu, *et al.*, *Adv. Funct. Mater.*, 2024, **34**(8), 2311773.
13 J. R. Luo, L. Xu, Y. N. Yang, S. Huang, Y. J. Zhou, Y. Y. Shao, T. H. Wang, J. M. Tian, S. H. Guo and J. Q. Zhao, *et al.*, *Nat. Commun.*, 2024, **15**(1), 6471.
14 D. Q. Cai, H. Y. Cheng, J. L. Yang, H. Liu, T. Xiao, X. Liu, M. H. Chen and H. J. Fan, *Energy Environ. Sci.*, 2024, **17**(21), 8349–8359.
15 Y. Q. Lv, M. Zhao, Y. D. Du, Y. Kang, Y. Xiao and S. M. Chen, *Energy Environ. Sci.*, 2022, **15**(11), 4748–4760.
16 K. L. Guan, L. Tao, R. Yang, H. N. Zhang, N. Z. Wang, H. Z. Wan, J. Cui, J. Zhang, H. B. Wang and H. Wang, *Adv. Energy Mater.*, 2022, **12**(9), 2103557.
17 J. R. Luo, L. Xu, Y. J. Zhou, T. R. Yan, Y. Y. Shao, D. Z. Yang, L. Zhang, Z. Xia, T. H. Wang and L. Zhang, *et al.*, *Angew. Chem., Int. Ed.*, 2023, **62**(21), 2302302.
18 Y. X. Lin, Y. Li, Z. X. Mai, G. Z. Yang and C. X. Wang, *Adv. Energy Mater.*, 2023, **13**(38), 2301999.
19 T. Xiao, J. L. Yang, B. Zhang, J. W. Wu, J. L. Li, W. J. Mai and H. J. Fan, *Angew. Chem., Int. Ed.*, 2024, **63**(8), 11.
20 H. M. Yang, K. Y. Zhu, W. L. Xie and W. S. Yang, *ACS Nano*, 2025, **19**(1), 1433–1446.
21 K. Wang, H. T. Zhan, W. L. Su, X. X. Liu and X. Q. Sun, *Energy Environ. Sci.*, 2025, **18**(3), 1398–1407.
22 T. Li, A. Naveed, J. Z. Zheng, B. X. Chen, M. F. Jiang, B. Y. Liu, Y. Zhou, X. W. Li, M. R. Su and R. Q. Guo, *et al.*, *Angew. Chem., Int. Ed.*, 2025, **64**(21), e202424095.
23 J. Yang, Z. Q. Han, Z. Q. Wang, L. Y. Song, B. S. Zhang, H. M. Chen, X. Li, W. M. Lau and D. Zhou, *Adv. Sci.*, 2023, **10**(22), 2301785.
24 Z. M. Yang, Y. L. Sun, S. T. Deng, H. Tong, M. Q. Wu, X. B. Nie, Y. F. Su, G. J. He, Y. H. Zhang and J. W. Li, *et al.*, *Energy Environ. Sci.*, 2024, **17**(10), 3443–3453.
25 C. Wu, Y. F. Pan, Y. C. Jiao and P. Y. Wu, *Angew. Chem., Int. Ed.*, 2025, 2423326.
26 L. M. Suo, O. Borodin, T. Gao, M. Olguin, J. Ho, X. L. Fan, C. Luo, C. S. Wang and K. Xu, *Science*, 2015, **350**(6263), 938–943.
27 N. Zhang, X. Y. Chen, M. Yu, Z. Q. Niu, F. Y. Cheng and J. Chen, *Chem. Soc. Rev.*, 2020, **49**(13), 4203–4219.
28 K. Xu, *Chem. Rev.*, 2014, **114**(23), 11503–11618.
29 C. Y. Yang, J. Chen, T. T. Qing, X. L. Fan, W. Sun, A. von Cresce, M. S. Ding, O. Borodin, J. Vatamanu and M. A. Schroeder, *et al.*, *Joule*, 2017, **1**(1), 122–132.
30 T. Xiao, J. L. Yang, B. Zhang, J. W. Wu, J. L. Li, W. J. Mai and H. J. Fan, *Angew. Chem., Int. Ed.*, 2024, **63**(8), e202318470.
31 H. W. Zhang, Y. Zhong, J. B. Li, Y. Q. Liao, J. L. Zeng, Y. Shen, L. X. Yuan, Z. Li and Y. H. Huang, *Adv. Energy Mater.*, 2023, **13**(1), 2203254.
32 Z. M. Zhao, J. N. Lai, D. T. Ho, Y. J. Lei, J. Yin, L. Chen, U. Schwingenschlögl and H. N. Alshareef, *ACS Energy Lett.*, 2022, **8**(1), 608–618.
33 L. Yu, J. Huang, S. J. Wang, L. H. Qi, S. S. Wang and C. J. Chen, *Adv. Mater.*, 2023, **35**(21), 2210789.
34 Y. Q. Lv, C. Y. Huang, M. Zhao, M. Z. Fang, Q. W. Dong, W. Q. Tang, J. T. Yang, X. X. Zhu, X. J. Qiao and H. F. Zheng, *et al.*, *J. Am. Chem. Soc.*, 2025, **147**(10), 8523–8533.
35 Y. Xu, K. Chen, M. Xu, Y. Li, Q. Wu, S. Li, C. Xie, Y. Li, H. Xie and J. Huang, *Energy Environ. Sci.*, 2025, **18**(3), 1560–1571.
36 C. Yuan, J. Xiao, C. Liu and X. Zhan, *J. Mater. Chem. A*, 2024, **12**(30), 19060–19068.
37 M. Q. Wu, Y. L. Sun, Z. M. Yang, S. T. Deng, H. Tong, X. B. Nie, Y. F. Su, J. W. Li and G. L. Chai, *Angew. Chem., Int. Ed.*, 2024, **63**(43), 2407439.
38 T. Lu and F. W. Chen, *J. Comput. Chem.*, 2012, **33**(5), 580–592.
39 J. Zhang and T. Lu, *Phys. Chem. Chem. Phys.*, 2021, **23**(36), 20323–20328.
40 T. Lu, *J. Chem. Phys.*, 2024, **161**(8), 082503.

